Journal of Molecular Spectroscopy 264 (2010) 43–49

Contents lists available at ScienceDirect

Journal of Molecular Spectroscopy

journal homepage: www.elsevier.com/locate/jms

# Extended analysis of hydroxyacetone in the torsional ground state

Rogier Braakman [a,*], Brian J. Drouin [b], Susanna L. Widicus Weaver [c], Geoffrey A. Blake [d]

[a] Division of Chemistry and Chemical Engineering, California Institute of Technology, Pasadena, CA 91125, USA
[b] Jet Propulsion Laboratory, California Institute of Technology, Pasadena, CA 91109-8099, USA
[c] Department of Chemistry, Emory University, Atlanta, GA 30322, USA
[d] Division of Geological and Planetary Sciences, California Institute of Technology, Pasadena, CA 91125, USA

ARTICLE INFO

*Article history:*
Received 4 August 2010
Available online 17 September 2010

*Keywords:*
Rotational spectroscopy
Internal rotation
Torsion–rotational coupling

ABSTRACT

The torsion–rotation spectrum of hydroxyacetone presents a highly challenging analysis problem in molecular physics. Continuing analyses of this species are compelling due to a nascent interest from astronomers, who believe hydroxyacetone may link a variety of organic chemical families observed in the interstellar medium (ISM). Recent work has demonstrated the difficulties in analysis of the millimeter spectrum, and the modestly weaker spectrum in this region has not afforded an ISM detection. We present an extension of the laboratory measurements and analysis up to the room temperature Boltzmann peak near 300 GHz, thus providing sufficient coverage to examine the ISM for the strongest features expected in star-forming hot cores. Even without subsequent detection, searches for the stronger features will produce the lowest possible upper limits of this elusive species.



## 1. Introduction

It has become increasingly clear that a stronger coupling between grain-surface and gas-phase chemistry is needed to explain the complex chemistry observed in dense molecular clouds in the interstellar medium (ISM). Furthermore, much remains to be understood about the relative contributions of various energetic pathways that drive the chemical processing of ices. One idea that has received increasing attention over the past few years is the formation of radical species in the quiescent, pre-collapse phase of an interstellar cloud, followed by reactions between these species as the grains are heated in the warm-up phase associated with core collapse and star-formation [1,2]. One route by which more complex species are formed is by single atom additions to abundant grain mantle constituents, CO molecules for example, initiated by the tunneling of hydrogen atoms, a process previously argued to be the only significant grain-surface pathway in quiescent clouds due the very low temperatures that prevail [3].

The second process now also thought to play an important role in the formation of radical species is the cleavage of molecular bonds by supra-thermal electrons that are released in the collision of highly energetic (>MeV) cosmic rays with dust grains. Both the models that include these two processes [1,2] and experimental studies of the processing of ice analogs with thermal electrons [4] have shown, for example, an overabundance in the formation of methyl formate versus its structural isomers acetic acid and glycolaldehyde, a trend that is not well explained by gas phase chemical models, yet widely observed in the interstellar medium (ISM) [5]. In order to disentangle the relative contributions of these and other pathways (e.g. UV photolysis) and better understand the complex web of reactions that drive interstellar chemistry, further observations and systematic comparisons of structurally related molecules are needed. The focus of this paper is hydroxyacetone ($HOCH_2COCH_3$), a structural intermediate between glycolaldehyde ($HOCH_2COH$) and the 3C sugar dihydroxyacetone ($HOCH_2COCH_2OH$, DHA), a compound widely observed in the soluble organic fraction of carbonaceous chondrites. Both glycolaldehyde and DHA have been the focus of previous observational studies [6–9], and we began preliminary laboratory/observational work on hydroxyacetone with these motivations in mind [10,11].

Our initial observational search for hydroxyacetone at $\lambda = 1.3$ mm with the Caltech Submillimeter Observatory (CSO, atop Mauna Kea) was unsuccessful [11], and while further work on the molecule was ongoing at Caltech, a detailed 3 mm survey using the SubMillimeter Telescope (SMT, at Mount Graham) confirmed it to be below detection limits [12]. After an initial tentative detection [8], a similarly detailed study of DHA showed this molecule to be undetected as well [9]. Thus, little interpretation can be made about the interstellar chemistry of these species beyond than the constraints on chemical models provided by the observational upper limits. However, the detection limits for complex species using the Herschel Space Observatory, the Atacama Large Millimeter Array (ALMA), and the Stratospheric Observatory for Far-Infrared Astronomy (SOFIA) are expected to be substantially lower

* Corresponding author. Present address: Santa Fe Institute, Hyde Park Road 1399, Santa Fe, NM 87501, USA.
*E-mail address:* rogier@santafe.edu (R. Braakman).

0022-2852/$ - see front matter © 2010 Elsevier Inc. All rights reserved.
doi:10.1016/j.jms.2010.09.003

than those achievable with ground-based 10-meter single dishes, and so these new facilities may well permit the detection of hydroxyacetone, DHA, and related species and thus permit a reconsideration of their chemistry.

The very high frequencies to which Herschel and ALMA have access place stringent demands on the quality of laboratory fits to the spectra of molecules such as hydroxyacetone. Thus, even though a previous millimeter-wave study of this molecule characterized the spectrum to $J_{max} = 30$ and $K_{a,max} = 12$ in the ground torsional state, an extrapolation of this analysis of the rotational–torsional spectrum of hydroxyacetone to the higher frequencies and quantum numbers that characterize transitions in the Herschel/ALMA submillimeter windows is fraught with uncertainty. Indeed, even a modest extension of the previous analysis from $\lambda = 3$ to 1 mm, where the lines are expected to be substantially stronger, results in line uncertainties that are larger than the typical spacing between features in the spectra of molecule rich hot cores such as Sgr B2(N).

The barrier to internal rotation of the methyl top in hydroxyacetone $V_3$ is only 65 $cm^{-1}$, which gives a reduced barrier of $s = 5.5$ ($s = 4V_3/9F$, where $F$ is the rotational constant of the methyl top). In this low-barrier regime, the $A - E$ splitting is on the order of the spacing between rotational levels, and in combination with asymmetry splitting, can make even assignments challenging – much less quantitative fits of the spectrum to experimental precision. In addition, the low barrier drives an effective coupling between the internal rotation of the top and overall rotation of the molecule, leading to many higher order off-diagonal terms in the Hamiltonian [13]. The combination of these effects makes the analysis of the torsion–rotation spectrum of hydroxyacetone a compelling spectroscopic problem, one that can aid in the continued quest of understanding the effects of internal rotation on rotational spectra of asymmetric molecules.

In our initial characterization of the spectrum of hydroxyacetone, difficulties in fitting the transitions of the $E$ state led to ambiguous observational results [11]. In a recent study [12], henceforth AP06, several microwave transitions from the initial microwave work on this molecule [14] were remeasured. The new frequencies led to significant revisions in the microwave assignments, and allowed a global fit to experimental accuracy for low to moderate $J$-values, and created an opportunity for us to revisit the problem. Furthermore, we have used hydroxyacetone as a test case to make several modifications to the SPFIT/SPCAT program suite developed by H.M. Pickett at JPL [18] in order to simplify the internal axis modeling of low-barrier internal rotation problems. This general and highly flexible program suite forms the core of the most widely used THz catalog available to astronomers and atmospheric scientists, and so an improved model and fitting procedure for low barrier internal rotors has much wider applicability than simply the present study of one compound.

The front-end program IAMCALC (Internal Axis Method Calculator) has recently been released as part of the CALPGM program suite (for further details see http://spec.jpl.nasa.gov). This program creates torsion–rotation operators through periodic solutions to the Mathieu equation which are then represented in the SPFIT/SPCAT programs as Fourier series (in energy and rotation operators) and off-diagonal torsional couplings (between specifically defined states whose symmetries match the torsional levels and sublevels) from user defined values such as barrier height and $\rho$ value. These parameters are then adjusted iteratively through each program to optimize both the spectral fit and the periodic solutions of the torsional problem. Used in tandem, the IAMCALC/SPFIT program suite is similar to the BELGI (BELGian Internal rotor) program developed by Kleiner [15], but there are a number of notable differences that must be considered when comparing results from these two packages. First, the open definition of parameters in IAMCALC/SPFIT allows very high order interactions to be modeled, whereas BELGI is limited to a pre-defined set of input parameters. Next, the IAMCALC basis may be chosen to be simple functions of $K$, rather than the Fourier expansions, thus allowing an accurate sampling of energy values near avoided crossings and/or cusps. Finally, the programs utilize separate definitions for the fundamental torsional operator, $P_\gamma$, which, in IAMCALC, is always Hermitian, $P_\gamma - \rho P_a$, but used in this form only for the definition of $F$ in BELGI – higher order terms in BELGI truncate the expression by elimination of $\rho P_a$. This latter difference requires either special parameter definitions for consistency between BELGI and IAMCALC, or a post-fit parameter transformation to compare the fitted values.

## 2. Experimental

Scans covering several millimeter and sub-millimeter spectral bands were measured as part of this work, providing a more extensive data set of the rotation–torsion spectrum of hydroxyacetone. The 91–120 and 275–350 GHz regions were recorded on the Caltech flow cell spectrometer; while the 230–250 GHz, 425–435 GHz regions, and a small window around 360 GHz were recorded using the JPL flow cell spectrometer. An example scan is shown in Fig. 1. Both instruments are similar in general setup and have been described in detail elsewhere [16,17]. Briefly, both consist of a fully computer controlled, swept frequency microwave (12–20 GHz) synthesizer followed by a series of fixed tuned harmonic multipliers and amplifiers that upconvert the microwave radiation into the desired band. The high frequency harmonics are then sent through a gas cell through which the sample flows at constant pressure. Radiation exiting the cell is then sampled with either a room temperature Schottky diode detector or a LHe-cooled InSb detector. The signal is ultimately recorded as a 2nd derivative lineshape using a lock-in amplifier set to the 2nd harmonic of the frequency modulation. In both experiments a flask of high purity hydroxyacetone, purchased from Sigma–Aldrich, was attached to the flow cell, and a sample pressure of 10–30 mTorr was maintained in a steady flow provided by use of a rotary vane pump.

## 3. Results and data analysis

Data were assigned in a boot-strap method using the IAMCALC/SPFIT/SPCAT program suite [18], in conjunction with the Sub-Millimeter Analysis Program (SMAP, also available at [18]). Further assignments were later made using Loomis–Wood visualization plots in the Computer Aided Assignment of Asymmetric Rotor Spectra (CAAARS) program suite [19]. The spectrum of hydroxyacetone exhibits several interesting trends, mainly due to asymmetry and internal rotation ($A$–$E$) splittings, that both aided our assignment of the spectrum and gave indications of the underlying physics of the rotation–torsion motions of the molecule. The first and most obvious of these trends is a series of collapsing quartets, similar to other asymmetric molecules with large dipole moments along two or more principle axes, such as lactic acid [20]. Both hydroxyacetone and lactic acid, for example, have significant dipole moments along the $a$- and $b$-inertial axes (lactic acid: $\mu_a = 1.44$ D, $\mu_b = 1.83$ D [20], hydroxyacetone: $\mu_a = 2.22$ D, $\mu_b = 2.17$ D [14]), and both molecules possess nearly degenerate pairs of $K_a$ levels at low $K_a$. This results in two, overlapping, $a$- and $b$-type asymmetry doublets, together making up the prominent quartet feature, examples of which can be seen in Fig. 2. The asymmetry splitting in these quartets decreases with $J$ for a given $K_a$, giving a single intense line at high $J$. Additionally, the asymmetry splitting increases with $K_a$, resulting in the collapse of the quartet at increasingly higher values of $J$. This trend, also illustrated

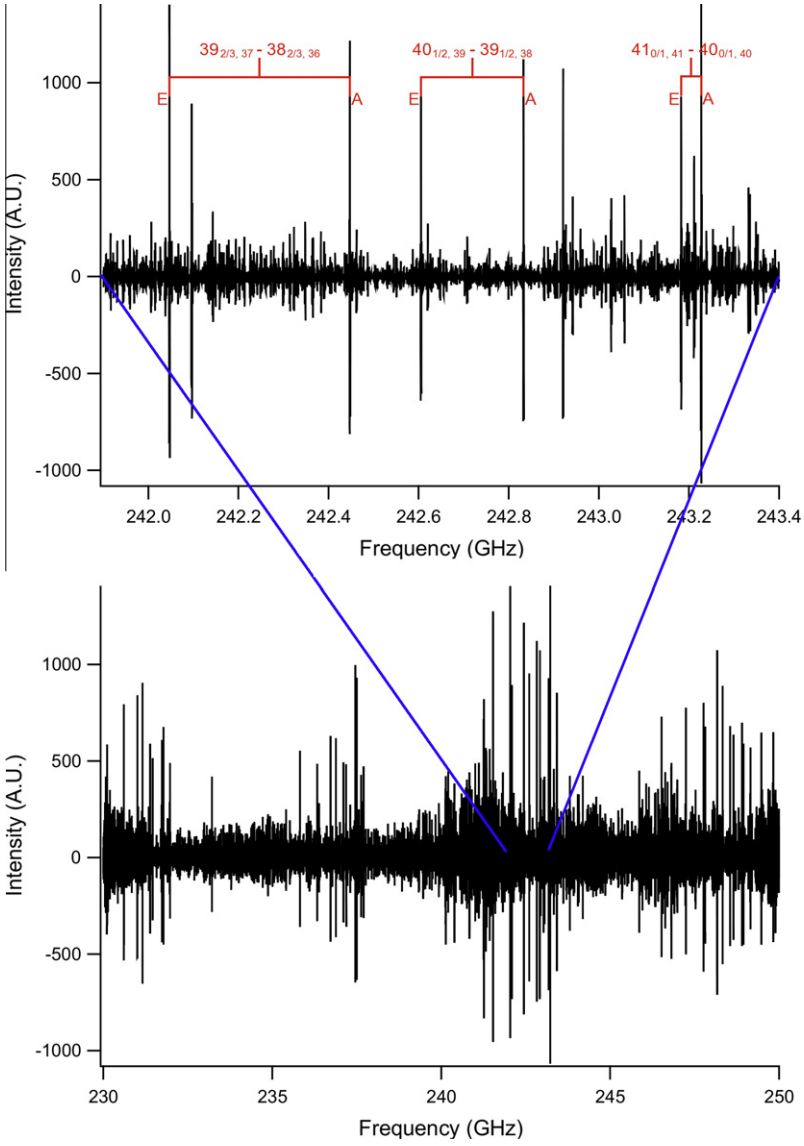


**Fig. 1.** A scan of the rotational spectrum of hydroxyacetone from 230 to 250 GHz. Data were recorded as a 2nd derivative line shape in FM mode. Strong $^{a}$R branches can be seen every ~5.7 GHz, and the internal structure of one such branch is shown in the inset. The most intense features arise from low-$K_a$ transitions in which the asymmetry splitting has lifted, summing the individual intensities and resulting in a single intense feature standing out from the rest of the spectrum (this coalescing pattern is detailed in Fig. 2). As $K_a$ increases, these lines can be seen walking off to lower frequencies, with the $41_{0/1,41} - 40_{0/1,40}$ line on the high frequency end of the scan and the $39_{2/3,37} - 38_{2/3,36}$ line on the low frequency end. The inset also shows the results of the internal rotation of the methyl group in the form of an $A - E$ splitting, with $E$ state companion for each line offset to lower frequency. The $A - E$ splitting increases with $K_a$, the $E$ state spectrum essentially walking off to lower frequencies faster than the $A$ state.

in Fig. 2, eventually makes it impossible to trace the quartet pattern in the spectrum. Here $K_a = 6, 7$ is the highest $K_a$ for which this pattern is still obvious in our data. At higher values of $K_a$, the splitting becomes so large that it is now pairs of $K_c$ levels with the same value of $K_a$ that become nearly degenerate, giving the more traditional asymmetry doublets with patterns opposite from before: the splitting increases with $J$ and decreases with $K_a$. In this case, $a$- and $b$-type doublets no longer overlap, giving somewhat less prominent, though still distinctive and intense, doublets.

The second main pattern in the spectrum is the $A - E$ splitting arising from the internal rotation of the methyl top. Due to the low barrier of hydroxyacetone, the $A - E$ splitting is quite large, often significantly larger than the asymmetry splitting. Nevertheless, the general patterns of the $E$ state spectrum are similar to that of the $A$ state, with collapsing quartets also being the most prominent features identifiable, albeit with smaller splitting(s). The $E$ quartet splitting is consistently ~60–65% of that in the $A$ state, allowing a relatively straight-forward mapping of the $E$ state transitions relative to the $A$ state transitions once the latter are assigned. The $A - E$ splitting increases regularly with $K_a$, from ~40 to 50 MHz for the $K_a = 0, 1$ quartet to approximately 1 GHz at $K_a = 6, 7$, with relatively small variations as a function of $J$ within the $K_a$ stacks.

In addition to using these patterns to confirm the assignment of the majority of the lines in the fit, the CAAARS program and its Loomis–Wood visualization was used to further expand the data set, in particular for transitions of high $J$ where the quartet pattern is no longer apparent and for assignment of various Q branches throughout the spectrum.

In all, over 1100 new transitions in the ground state rotation–torsion spectrum of hydroxyacetone, up to frequencies of 430 GHz, were assigned using the methods described above. The full data set includes $a$-type transitions up to $J = 75$ and $K_a = 16$ and $b$-type transitions up to $J = 75$ and $K_a = 18$ in the $A$ state, and $J = 75$, $K_a = 13$ and $J = 75$, $K_a = 10$ for $a$- and $b$-type

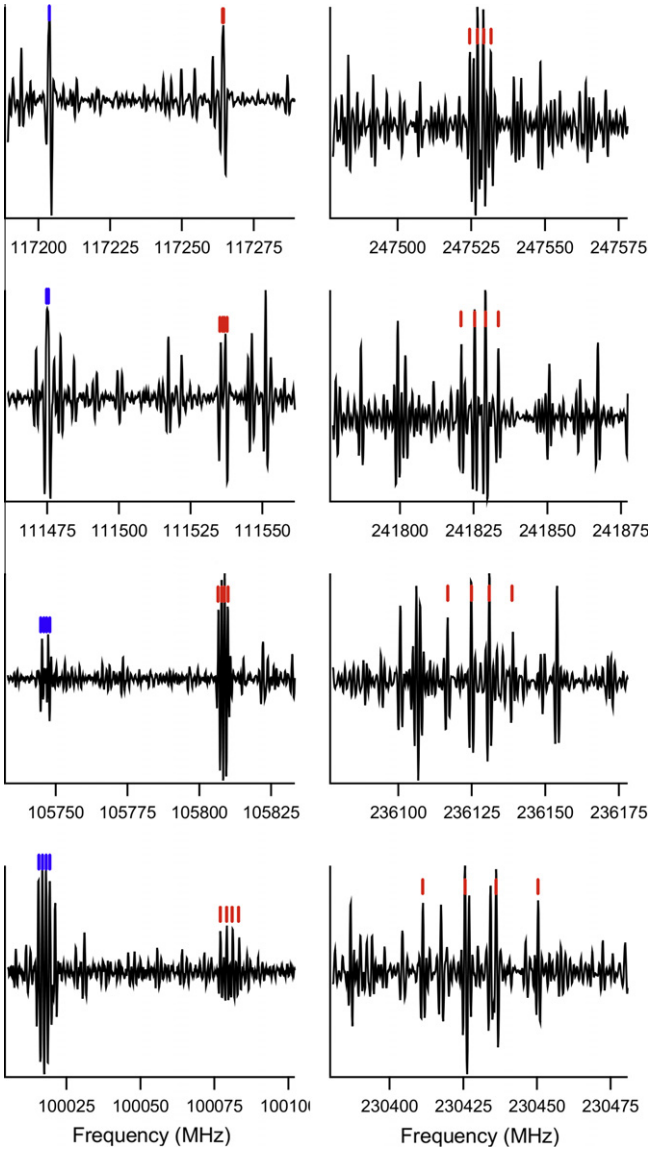


**Fig. 2.** Loomis–Wood plots showing the prominent asymmetry quartet pattern. The left panels show the $K_a = 0, 1$ quartet in both the *A*-state (red) and the *E*-state (blue) from $J_{upper} = 17$—20. It can be seen that the *E*-state has a lower asymmetry splitting, at about ~60–65% of that of the *A*-state. The right panels show the $K_a = 4, 5$ quartet in the *A*-state, from $J_{upper} = 36$—39. Here the *E*-state is not shown, as the $A - E$ splitting has increased from about 60 MHz for the $K_a = 0, 1$ quartet to over 700 MHz for these states. Together, these plots show the lifting of the asymmetry splitting as *J* increases, resulting in intense lines that stand out from the rest of the spectrum (also seen in Fig. 1). The asymmetry splitting further increases with $K_a$, the $K_a = 4, 5$ quartet coalesces at over 20 units of *J* and 130 GHz higher than the $K_a = 0, 1$ quartet. (For interpretation of the references to color in this figure legend, the reader is referred to the web version of this article.)

transitions, respectively, in the *E* state. The increased torsional interaction in the *E* state make it more difficult to characterize, hence the smaller range in $K_a$. This is also the reason 'only' 472 new lines were assigned in the *E* state versus 677 new lines in the *A* state. The new data set also includes several nearly complete *Q* branches up to $K_a = 10$ for both the *A* and *E* states in the 91–120 GHz region that were previously unassigned [12], and represents a significant increase in quantum number coverage. Previous spectral analyses of hydroxyacetone were limited to values of $J = 30$ and $K = 12$, including only a handful of transitions above $K = 7$ for *b*-types in the *A* state, and only 2 transitions above $K = 5$ in the *E* state [12]. The newly assigned lines were ultimately combined with the AP06 set to give a total of 2300 transitions. In AP06, the line list from Kattija–Harmony (1980) was reassessed, and assignments that were determined to be incorrect were either reassigned or removed from the set. Two additional transitions, left out of the AP06 fit, were reassigned here and added to the list: the 30997.800 MHz line was identified as the $5_{1,5} - 4_{1,4}$ *E* state transition, and the 34514.380 MHz line was identified as the $8_{3,5} - 8_{2,6}$ *E* state transition [14].

Fitting was done using the SPFIT/SPCAT program suite, including the IAMCALC front-end that uses the Internal Axis Method (IAM) to analyze the effects of internal rotation. Initial fits utilized the parameter and data set of AP06 [9] as a starting point. This allowed further assignment and expansion of the analysis through an iterative process. Although the IAM basis used in this procedure includes excited torsional states implicitly, the transitions predicted for these states did not conform to any recognizable patterns in the unassigned portions of the recorded spectra. It is likely that the extremely low barrier of hydroxyacetone makes it a poor choice for a global torsional analysis such as that performed recently on methanol [21] or acetaldehyde [22]. In these latter two studies the global torsional analysis is valid up to approximately $v_t = 3$, at which point the higher torsional states transition to a free-rotor situation instead of a low-barrier hindered rotor. Similarly, we believe that assignment of the $v_t > 0$ states of hydroxyacetone will require a different basis than that presented here and in AP06 [9].

Our analysis includes a total of 39 parameters, shown in Table 1. The numerical results of the analysis are complied in Table 2, which also lists the results of the AP06 analysis for comparison. Table 1 is presented in the format of [23] to show the order progression of the operators included in our analysis. Due to the differences in parameter definitions as described in the introduction (in the AP06 study the BELGI program suite was used) the parameters have been transformed to allow direct comparison. Lines with an obs–calc error of larger than 7 times the experimental uncertainty were removed from the fit. This truncation excluded approximately 60 transitions from the final fit, and resulted in a global rms of 120 kHz for the remaining lines, close to experimental uncertainty of ~100 kHz. The factor of 7 in the truncation was chosen somewhat arbitrarily, but was an attempt to balance the inclusion of as many lines as possible while simultaneously excluding those transitions for which the model was clearly breaking down. The excluded lines were consistently the highest *J* transitions within $K_a$ stacks for a particular type of transition, with the onset first appearing around $J = 50 - 55$ for the $K_a = 4, 5$ quartets and the divergence occurring at subsequently lower values of *J* for increasing $K_a$. Because the error progression in the divergence is smooth and also because these transitions were assigned using Loomis–Wood plots, we believe this to be due to breakdown in the model at high quantum numbers rather than a misassignment of lines. The great difficulty in assigning *Q* branches above $K_a = 10$, where the $K_a = 18 - 17$ *Q* branch in the *A* state is the only exception, also supports this conclusion. The excitation energies at which these divergences occur are at least 300—500 $cm^{-1}$, depending on $K_a$, and so all lines likely to be strong under hot core conditions are now predicted to essentially experimental precision. Based on the results of our analysis, an entry for hydroxyacetone was created for the JPL spectral line catalog, and can be found at http://spec.jpl.nasa.gov.

## 4. Discussion

The rotational spectrum of the ground vibrational state of hydroxyacetone has been characterized up to 435 GHz. A total of 2300 lines in both the *A* and *E* states were fit to a global model with 39 parameters. This is a significant increase in the number of

**Table 1**
Rotational, torsional and cross-terms determined for hydroxyacetone.

| Rotational operator | Torsional operator | | | | | | | | |
|---|---|---|---|---|---|---|---|---|---|
| | 1 | $\tilde{P}_\gamma^2$ | $\tilde{P}_\gamma P_a$ | $1-\cos 3\gamma$ | $\left\{\tilde{P}_\gamma^2, c\right\}$ | $\left\{\tilde{P}_\gamma P_a, c\right\}$ | $1-\cos 6\gamma$ | $\tilde{P}_\gamma^3 P_a$ | $P_\gamma^4$ |
| 1 | | $F$ | $-2\rho F$ | $V_3/2$ | | | | $k_3$ | |
| $P^2$ | $\frac{B+C}{2}$ | $G_v$ | $L_v$ | $F_v$ | | | | $k_{3J}$ | |
| $P_a^2$ | $A-\frac{B+C}{2}$ | | $k_1$ | $k_5$ | | | | $k_{3K}$ | |
| $P_b^2-P_c^2$ | $\frac{B-C}{4}$ | $c_1$ | $c_4$ | $c_2$ | | $c_{3a}$ | | $c_{3b}$ | |
| $\{P_a, P_b\}$ | $D_{ab}$ | $\Delta_{ab}$ | $\delta_{ab}$ | $d_{ab}$ | | | | | |
| $P^4$ | $-\Delta_J$ | $g_v$ | | $f_v$ | | | | | |
| $P^2P_a^2$ | $-\Delta_{JK}$ | | | | | | | | |
| $P_a^4$ | $-\Delta_K$ | | $l_k$ | | | | | | |
| $2P^2(P_b^2-P_c^2)$ | $-\delta_J$ | | | | | | | | |
| $\left\{P_a^2,(P_b^2-P_c^2)\right\}$ | $-\delta_K$ | | | | | | | | |
| $P_a^2\{P_a, P_b\}$ | $D_{abK}$ | | | | | | | | |
| $P^6$ | $\Phi_J$ | | | | | | | | |
| $P^4P_a^2$ | $\Phi_{JK}$ | | | | | | | | |
| $P^2P_a^4$ | $\Phi_{KJ}$ | | | | | | | | |
| $P_a^6$ | $\Phi_K$ | | | | | | | | |
| $2P^4(P_b^2-P_c^2)$ | $\phi_J$ | | | | | | | | |
| $P^2\left\{P_a^2,(P_b^2-P_c^2)\right\}$ | $\phi_{JK}$ | | | | | | | | |
| $\left\{P_a^4,(P_b^2-P_c^2)\right\}$ | $\phi_K$ | | | | | | | | |

parameters compared to previous studies [12], and is mainly required due to the large increase in both $J$ and $K_a$ coverage. This has allowed us to determine the rotational, torsional and rotational–torsional cross terms in the Hamiltonian to 8th order. As can be seen in Table 1, higher order terms were added in a consistent manner, always exhausting lower order possibilities before including higher order terms.

As to the breakdown of the model at higher $J$ within $K_a$ stacks, there are several possible reasons for this. First to consider are the excited torsional/vibrational states, which can interact with and perturb the ground state if they sufficiently low in energy. Hydroxyacetone has several low-lying excited states, most importantly the methyl torsion, which has been calculated to lie near 65 $cm^{-1}$ (but which is too weak to have been observed in Raman spectra), and the $CH_2OH$ torsion that has been measured at 80 $cm^{-1}$ [24]. Additional low-lying bands that are experimentally observed are the OCC in plane bending mode at 276 $cm^{-1}$ and the OH torsion at 330 $cm^{-1}$ [24], both of which could potentially impact the rotational spectrum of the ground state. The importance of these low-lying excited states is confirmed by the presence of many unassigned lines in our data with similar or larger intensity than the ground state. As these lines are currently unassigned, interactions with the excited states have not been explicitly included in our model. IAMCALC does assume a basis set including several excited states in predicting the parameters for the rotational Hamiltonian, but these are predicted internally in the program mainly as a consistency check, and more explicit assignments may be needed. Early on we attempted to include several of the remaining intense transitions into the fit; and while it was possible to assign several branches based on quartet patterns and using Loomis–Wood plots, the fit did not converge when these additional series were included. Additionally, the predictions for the excited state transitions using our first order model were not close to the spectral features observed, making the identification of the states to which the lines belong difficult. A more profitable route would likely be to return to the microwave region in order to measure the lowest $J$, $K_a$ lines in the excited states before attempting to fit the (sub)mm-wave lines.

A second effect that can also cause line shifts is due to local repulsive interactions when different $K$ stacks in a given torsional state approach or cross each other. With the high density of states for hydroxyacetone, this is certainly not an unlikely scenario. However, it is the consistent and more general breakdown of the model that leads us to believe this 'internal' $K$ stack effect is likely less important in characterizing the full rotational spectrum than are the excited torsional/vibrational states. Once the excited states have been included and the fit has been stabilized, further analysis and refinement should allow identification of $K$ stack effects if they indeed occur.

Even with the limitations of the model as discussed above, the present results provide a significant improvement in the overall description of the rotational–torsional spectrum of hydroxyacetone compared to previous studies, and demonstrate that the recent extensions of the SPFIT/SPCAT program suite now permit the quantitative analysis of low barrier (single) internal rotor spectra. The pure rotational assignments in the ground torsional state have been extended from $J = 30$ and $K_a = 12$ up to $J = 75$ and $K_a = 18$ in this study, and the rotational–torsional terms have been refined and extended up to 8th order, making hydroxyacetone one of the few asymmetric molecule/low barrier internal rotors for which such an extensive rotation-centrifugal distortion analysis exits. As noted above, the expanded fit is also a significant milestone in the use of SPFIT/SPCAT to study such systems, as the program suite proved capable, indeed highly successful, of fitting both $A$ and $E$ states in a single, global, model.

Finally, from an observational perspective, this study catalogs the vast majority of the important lines under hot core conditions by extending the assignments from 180 GHz up to 435 GHz. Thus, most of the windows available to the CSO and other similar (ground-based) observatories can now be used to search for transitions of hydroxyacetone. As has been discussed previously (e.g. [17,25]), simply predicting the frequencies of even the most well-described transitions can lead to unacceptable errors when large frequency extrapolations are required. These laboratory characterizations are therefore a crucial first step in exploring observational windows at $\lambda < 1$ mm. However, with both our initial attempts [11] and subsequent efforts at longer wavelengths (AP06) providing only upper limits on the column density, new single dish telescope observations over large spatial scales are not likely to meet with success. Given the compact nature of most

**Table 2**
Spectroscopic parameters for the ground vibrational state of hydroxyacetone.

| Operator | Parameter (units) | Value | |
|---|---|---|---|
| | | This work | AP06 |
| $\frac{1}{2}(1-\cos 3\gamma)$ | $V_3$ (cm$^{-1}$) | 65.3038 | 65.3560 |
| $P_\gamma^2$ | $F$ (MHz) | 158942 | 159118.2 |
| $P_\gamma P_a$ | $\rho$ (unitless) | 0.0587318 | 0.0587793 |
| $P^2$ | $(B+C)/2$ (MHz) | 3434.434(62) | 3439.8048 |
| $P_a^2$ | $A-(B+C)/2$ (MHz) | 6460.209(41) | 6439.3312 |
| $P_b^2-P_c^2$ | $(B-C)/4$ (MHz) | 285.733(33) | 286.5946 |
| $\{P_a,P_b\}$ | $D_{ab}$ (MHz) | 1097.364(213) | 1089.287 |
| $(1-\cos 3\gamma)P^2$ | $F_V$ (MHz) | −5.512(167) | −1.772 |
| $(1-\cos 3\gamma)P_a^2$ | $k_5$ (MHz) | 20.221(70) | 26.585 |
| $(1-\cos 3\gamma)(P_b^2-P_c^2)$ | $c_2$ (MHz) | −0.704(88) | −1.746 |
| $(1-\cos 3\gamma)\{P_a,P_b\}$ | $d_{ab}$ (MHz) | 2.80(60) | 12.696 |
| $P_\gamma^2P^2$ | $G_\nu$ (MHz) | −0.3396(168) | |
| $P_\gamma^2P_a^2$ | $k_2$ (MHz) | | 0.9809 |
| $P_\gamma^2(P_b^2-P_c^2)$ | $c_1$ (MHz) | 0.0205(88) | −0.03229 |
| $P_\gamma^2\{P_a,P_b\}$ | $\Delta_{ab}$ (MHz) | −0.392(65) | 0.4800 |
| $P_\gamma P_aP^2$ | $L_V$ (MHz) | 0.01772(19) | −0.00053 |
| $P_\gamma P_a^3$ | $k_1$ (MHz) | 0.0128(57) | 0.00174 |
| $P_\gamma P_a(P_b^2-P_c^2)$ | $c_4$ (MHz) | −0.0119(43) | −0.00015 |
| $P_\gamma P_a\{P_a,P_b\}$ | $\delta_{ab}$ (MHz) | −0.03239(228) | −0.08554 |
| $P_\gamma^3P_a$ | $k_3$ (MHz) | 2.331(117) | −0.1730 |
| $P^4$ | $-\Delta_J$ (kHz) | −0.8350(74) | −0.8399 |
| $P^2P_a^2$ | $-\Delta_{JK}$ (kHz) | 9.91(40) | 8.984 |
| $P_a^4$ | $-\Delta_K$ (kHz) | −27.19(62) | −29.58 |
| $P^2(P_b^2-P_c^2)$ | $-\delta_J$ (kHz) | −0.2515(37) | −0.24274 |
| $\left\{P_a^2,(P_b^2-P_c^2)\right\}$ | $-\delta_K$(kHz) | 2.743(150) | 2.599 |
| $P_a^2\{P_a,P_b\}$ | $D_{abK}$ (kHz) | 16.85(59) | 18.41 |
| $\{P_\gamma P_a,(1-\cos 3\gamma)\}(P_b^2-P_c^2)$ | $c_{3a}$ (kHz) | −0.01368(54) | |
| $P_\gamma^3P_aP^2$ | $k_{3J}$ (kHz) | 11.27(64) | |
| $P_\gamma^3P_a^3$ | $k_{3K}$ (kHz) | −47.4(34) | |
| $P_\gamma^3P_a(P_b^2-P_c^2)$ | $c_{3b}$ (kHz) | −8.697(192) | |
| $(1-\cos 3\gamma)P^4$ | $f_\nu$ (kHz) | −0.04695(110) | |
| $P_\gamma^2P^4$ | $g_\nu$ (Hz) | 2.907(58) | |
| $P_\gamma P_a^5$ | $l_k$ (kHz) | 0.0536(43) | |
| $P^6$ | $\Phi_J$ (Hz) | 0.004223(168) | |
| $P^4P_a^2$ | $\Phi_{JK}$ (Hz) | −0.0298(77) | |
| $P^2P_a^4$ | $\Phi_{KJ}$ (Hz) | 1.337(49) | |
| $P_a^6$ | $\Phi_K$ (Hz) | −1.396(61) | |
| $2P(P_b^2-P_c^2)$ | $\phi_J$ (Hz) | 0.002134(84) | |
| $P^2\left\{P_a^2,(P_b^2-P_c^2)\right\}$ | $\phi_{JK}$ (Hz) | −0.0432(33) | |
| $\left\{P_a^4,(P_b^2-P_c^2)\right\}$ | $\phi_K$ (Hz) | 1.1845(297) | |

hot core sources, interferometric observations with either the Combined Array for Research in Millimeter Astronomy (CARMA) in the short term or, especially, ALMA once it is fully operational in 2013 (shared risk observations with roughly a quarter of ALMA will begin in 2011) should provide much better detection limits through their larger collecting area and ability to spatially filter out the extended emission from simpler molecules. Alternatively, the line confusion can be largely reduced by moving to THz frequency observations with Herschel or SOFIA. If such observations ultimately do lead to a detection of torsionally excited hydroxyacetone, the present analysis will be of use in further detailed laboratory analyses of the torsional spectrum and in the global fitting of confusion-limited surveys that provide the best platform for the identification of new species [26].

## Acknowledgments

R.B. acknowledge J. Hougen at NIST for useful discussions on internal axis system (IAM) methods. The efforts of R.B. and G.A.B. were funded in part by the NASA SARA program, Grant NAG5-13457. Portions of this paper present research carried out at the Jet Propulsion Laboratory, California Institute of Technology, under contract with the National Aeronautics and Space Administration.

## References

[1] R. Garrod, E. Herbst, A&A 457 (2006) 927.
[2] R. Garrod, S. Widicus Weaver, E. Herbst, ApJ 682 (2008) 283.
[3] S. Charnley, ApJ 562 (2001) 99.
[4] C. Bennet, R. Kaiser, ApJ 661 (2007) 899.
[5] J. Hollis, S. Vogel, L. Snyder, P. Jewell, F. Lovas, ApJ 554 (2001) 81.
[6] J. Hollis, F. Lovas, P. Jewell, ApJ 540 (2000) L107.
[7] J. Hollis, F. Lovas, P. Jewell, A. Remijan, ApJ 613 (2004) L45.
[8] S. Widicus Weaver, G. Blake, ApJ 624 (2005) L33 (erratum: 63, L163).
[9] A. Apponi, D. Halfen, L. Ziurys, J. Hollis, A. Remijan, F. Lovas, ApJ 643 (2006) L29.
[10] R. Braakman, M.Sc. Thesis, University of Amsterdam, 2003.
[11] R. Braakman, B. Drouin, S. Widicus Weaver, G. Blake, in: 60th OSU Int. Symp. Mol. Spec., 2005, pp. RA07.
[12] A. Apponi, S. Hoy, D. Halfen, L. Ziurys, M. Brewster, ApJ 652 (2006) 1787.
[13] C. Lin, J. Swalen, Rev. Mod. Phys. 31 (1959) 841.
[14] M. Kattija-Ari, M. Harmony, Int. J. Quant. Chem. Symp. 14 (1980) 443.

[15] J. Hougen, I. Kleiner, M. Godefroid, J. Mol. Spectrosc. 163 (1994) 559.
[16] B. Drouin, F. Maiwald, J. Pearson, Rev. Sci. Instrum. 76 (2005) 093113.
[17] S. Widicus Weaver, R. Braakman, D. Kent, G. Blake, J. Mol. Spectrosc. 224 (2004) 101.
[18] H. Pickett, F. Poynter, E. Cohen, M. DeLitsky, J. Pearson, H. Muller, J. Quant. Radiat. Trans. 60 (1998) 883.
[19] I. Medvedev, M. Winnewisser, B. Winnewisser, F. DeLucia, E. Herbst, J. Mol. Spectrosc. 229 (2005) 742.
[20] L. Pszczolkowski, E. Bialkowski-Jaworski, Z. Kisiel, J. Mol. Spectrosc. 234 (2005) 106.
[21] L.-H. Xu, J. Fisher, R. Lees, H. Shi, J. Hougen, J. Pearson, B. Drouin, G. Blake, R. Braakman, J. Mol. Spectrosc. 251 (2008) 305–3113.
[22] I. Kleiner, F. Lovas, M. Godefroid, J. Phys. Chem. Ref. Data 25 (1996) 1113–1210.
[23] K. Ogata, H. Odashima, K. Takagi, S. Tsunekawa, J. Mol. Spectrosc. 225 (2004) 14.
[24] V. Mohacek-Grosev, Spectrochim. Acta A 61 (2005) 477.
[25] D. Halfen, A. Apponi, N. Woolf, R. Polt, L. Ziurys, ApJ 639 (2006) 237.
[26] I. Medvedev, F. DeLucia, ApJ 656 (2007) 621.